

# Misorientation dependence of discontinuous precipitation in Cu-Be alloy bicrystals

R. MONZEN, H. SHIGEHARA, K. KITA

*Department of Mechanical Systems Engineering, Kanazawa University,  
2-40-20 Kodatsuno, Kanazawa 920-8667, Japan*

*E-mail: monzen@t.kanazawa-u.ac.jp*

The boundary-dependent discontinuous precipitation (DP) for various [001] symmetric tilt boundaries in Cu–5.2 at% Be alloy bicrystals has been examined in the temperature range 523–698 K. The precipitate phase maintains a constant interlamellar spacing under isothermal growth conditions. The interlamellar spacing increases with an increase in temperature. The incubation period  $\tau$  to initiate DP and cell growth rate for DP against misorientation angle diagrams show local peaks and cusps at the same misorientation angles. The positions of the peaks and cusps agree with those of cusps in the boundary energy against misorientation diagram. The formation and growth of DP occur more easily at higher-energy boundaries. A detailed kinetic analysis of the experimental data using the models by Turnbull and Petermann–Hornbogen has enabled the determination of the grain-boundary diffusivity of Be along each boundary in the temperature range studied. A close correlation is found between the diffusivity and the energy of boundaries. A higher-energy boundary has a higher diffusivity with a smaller activation energy and a smaller pre-exponential factor. © 2000 Kluwer Academic Publishers

## 1. Introduction

Discontinuous precipitation (DP) involves the formation of a solute-depleted matrix phase ( $\alpha$ ) and a precipitate phase ( $\gamma$ ) as a duplex transformation product behind a grain boundary advancing into a supersaturated matrix ( $\alpha_0$ ). This solid state phase transformation is so termed because the changes in orientation and composition between the matrix phases ( $\alpha$  and  $\alpha_0$ ) across the advancing boundary are discontinuous. The advancing boundary provides a short-circuit path of solute transport.

It is well known that the formation and growth of DP vary from boundary to boundary. This is because such factors as grain-boundary mobility and grain-boundary diffusion depend on the character of individual boundaries. For example, DP reaction is found to be more difficult for coincidence-site boundaries with low values of  $\Sigma$  compared with random boundaries [1–3]. In this study, we investigate systematically the formation and growth of DP at various [001] symmetric tilt boundaries in bicrystals of a Cu–5.2 at% Be alloy. To our knowledge, there has been no systematic study using orientation-controlled bicrystals to examine the influence of grain-boundary character on DP.

DP is a boundary-diffusion-controlled reaction. Thus, analysis of the steady-state DP reaction kinetics offers an indirect but convenient and reliable method of measuring the boundary chemical diffusivity in systems which undergo DP [4]. This approach has already been applied in a number of binary systems showing DP; for example, Zn–Al [5], Zn–Cu [6], Cu–Be [7], etc. The

present paper concerns a detailed kinetic analysis of DP and determination of the diffusivity of Be along individual [001] symmetric tilt boundaries of Cu–5.2 at% Be.

## 2. Experimental

Cu–5.2at%Be alloy ingots were prepared by melting of electrolytic Cu (99.99%) and Cu–13 at%Be master alloy in a high-purity alumina crucible under an Ar atmosphere. Bicrystals of this alloy containing various [001] symmetric tilt boundaries with misorientation angles  $\theta = 14\text{--}80^\circ$  were grown in a high-purity graphite mold by the Bridgman method using two seed crystals. Hereafter, the bicrystal with the misorientation angle  $\theta$  and its grain boundary will be expressed as  $\theta$  bicrystal and  $\theta$  boundary, respectively. After confirming by the X-ray Laue analysis that the actual misorientation angles were within  $\pm 1^\circ$  of the given angles, the bicrystals were homogenized at 1123 K and then spark-cut into specimen pieces of 1 mm  $\times$  15 mm  $\times$  15 mm. The specimens were solution-treated at 1073 K for 1 h in a vacuum, quenched into iced water and then aged at 523 K (800–1800 h), 573 K (48–240 h), 623 K (18–120 h), 648 K (18–90 h), 673 K (12–60 h), and 698 K (12–48 h) in a vacuum. A chemical analysis showed that the aged specimens contained  $5.2 \pm 0.02$ at%Be.

Quantitative metallographic measurements were performed by optical microscopy (OM) and scanning electron microscopy (SEM). The interlamellar spacing  $\lambda$  was determined by the method previously reported by

Tsubakino *et al.* [7, 8]. The uncertainty of the measured values of  $\lambda$  was within a few percent.

The foils for transmission electron microscopy (TEM) were thinned at 5 V in a twin-jet electropolisher using a 20% solution of phosphoric acid in water at about 280 K. TEM observations were carried out using a HITACHI H-9000NAR operating at 300 kV.

### 3. Results and discussion

#### 3.1. Microscopic observations and $\lambda$

The microstructure observed through OM and SEM revealed that the supersaturated solid solution  $\alpha_0$  decomposed into  $\alpha$  and  $\gamma$  phases at ageing temperatures in the range 523–698 K. Fig. 1 shows an example. At 723 K no DP reaction took place. During the course of isothermal precipitation, the  $\gamma$  phase maintained a constant value of  $\lambda$ . As shown in Fig. 2,  $\lambda$  did not depend essentially on the misorientation angle or boundary character, and increased with increasing temperature  $T$ . Extrapolation of the  $1/\lambda$  against  $T$  plot to  $1/\lambda = 0$  in Fig. 2 yields an  $x$ -axis intercept of  $T_{DP} = 723$  K. It should be pointed out that  $T_{DP}$  corresponds to the hypothetical situation where  $\lambda$  is infinite, signifying cessation of DP at  $T \geq T_{DP}$ . It can further be noted that  $T_{DP}$  in the present study is in reasonable agreement with the  $T_{DP}$  (=713 K) obtained from microscopic observations by Tsubakino *et al.* [7].

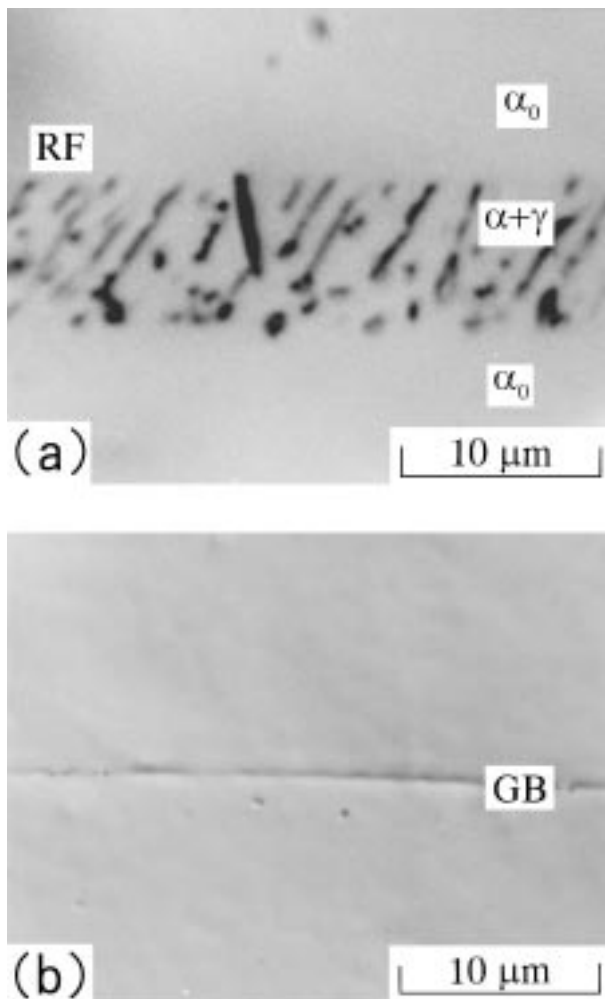


Figure 1 Optical micrographs of (a)  $\theta = 30^\circ$  and (b)  $\theta = 80^\circ$  bicrystals aged at 523 K for 1000 h. RF = reaction front, GB = grain boundary.

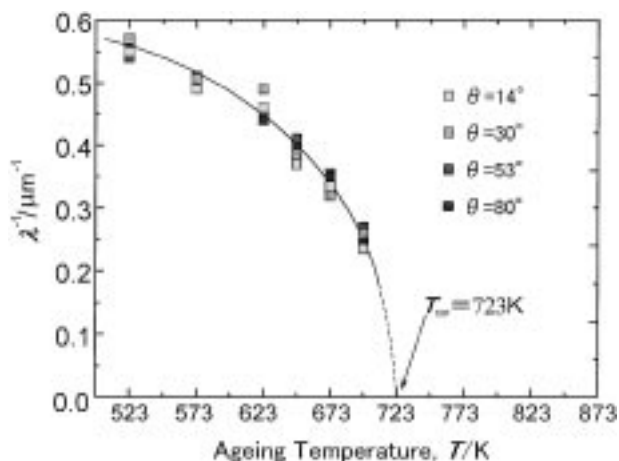


Figure 2 Variation of the reciprocal of  $\lambda$  as a function of temperature  $T$ .

Observations using TEM and selected-area electron diffraction patterns showed that no precipitates formed in the Cu matrix of in-grains during ageing at 523 and 573 K. On ageing at 623 K, the continuous precipitation of  $\gamma''$  phase occurred between 24 and 120 h. At 648 K  $\gamma'$  continuous precipitates were observed between 24 and 90 h. However, the cell growth rate of DP was unchanged and linear in spite of the formation of  $\gamma''$  or  $\gamma'$ . This is in agreement with the conclusion previously obtained by Tsubakino *et al.* [8] that fine  $\gamma''$  or  $\gamma'$  precipitates do not affect the cell growth. On ageing at 673 and 698 K, fine  $\gamma$  precipitates were observed eventually after 60 and 48 h, respectively, which are the longest ageing times. The existence of the  $\gamma$  precipitates did not change the cell growth rate.

#### 3.2. Formation and growth of cells

Fig. 1 shows optical micrographs of bicrystals with (a)  $\theta = 30^\circ$  and (b)  $\theta = 80^\circ$  [001] symmetric tilt boundaries after ageing at 523 K for 1000 h. The ageing produces no DP cell at the  $80^\circ$  boundary. It is clear that the DP reaction of the  $\gamma$  phase at the  $30^\circ$  boundary occurs more rapidly than that at the  $80^\circ$  boundary.

Fig. 3 shows the variation of cell width  $L$  with time  $t$  on ageing at 523 K for  $30^\circ$ ,  $53^\circ$  and  $63^\circ$  boundaries.

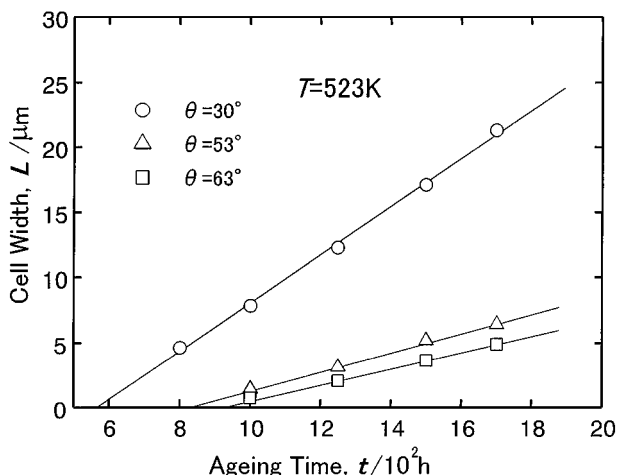


Figure 3 Variation of the cell width  $L$  at  $30^\circ$ ,  $53^\circ$  and  $63^\circ$  boundaries during ageing at 523 K.

A linear relationship exists between  $L$  and  $t$  for these boundaries. For all boundaries and ageing temperatures examined,  $L-t$  plots maintained such linearity. From the slope of the straight line drawn by the least-squares method, the growth rate of cell  $v$  can be obtained for each boundary and ageing temperature. The calculated values of  $v$  at 523 K are shown against the misorientation angle  $\theta$  in Fig. 4. The dependence of  $v$  on  $\theta$  is non-monotonous; several cusps exist. The variation of  $v$  with  $\theta$  at the other temperatures followed a similar trend. For all the boundaries,  $v$  increased monotonically as  $T$  rose, with a maximum at 698 K. It is also seen from Fig. 3 that the incubation period  $\tau$  to initiate DP (i.e. the intercept on the abscissa at  $L = 0$ ) is dependent strongly upon the misorientation angle. Fig. 5 shows  $\tau$  at 523 K against the misorientation.

The  $v-\theta$  and  $\tau-\theta$  diagrams show, respectively, local cusps and peaks near  $\theta = 28.1^\circ$  ( $\Sigma = 17$ ),  $\theta = 36.9^\circ$  ( $\Sigma = 5$ ),  $\theta = 53.2^\circ$  ( $\Sigma = 5$ ),  $\theta = 61.9^\circ$  ( $\Sigma = 17$ ) and  $\theta = 73.7^\circ$  ( $\Sigma = 25$ ). However, no cusps and peaks are seen at misorientation angles corresponding to relatively low- $\Sigma$  boundaries, such as  $\theta = 22.6^\circ$  ( $\Sigma = 13$ ) and  $\theta = 67.4^\circ$  ( $\Sigma = 13$ ), which can be inferred to show cusps and peaks according to the  $\Sigma$ -value criterion. On the other hand, the positions of cusps and peaks in the

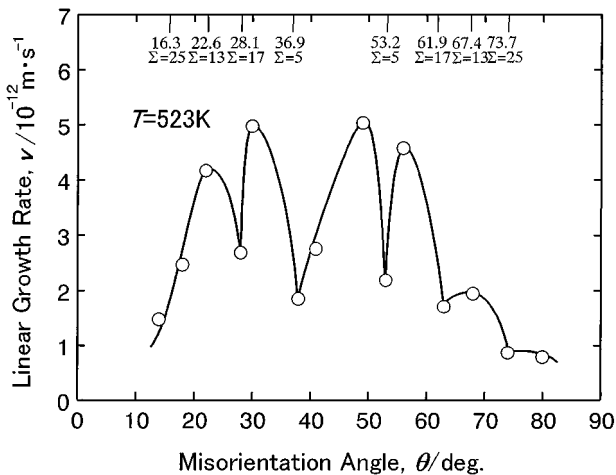


Figure 4 Cell growth velocity  $v$  at 523 K, plotted against the misorientation angle  $\theta$ .

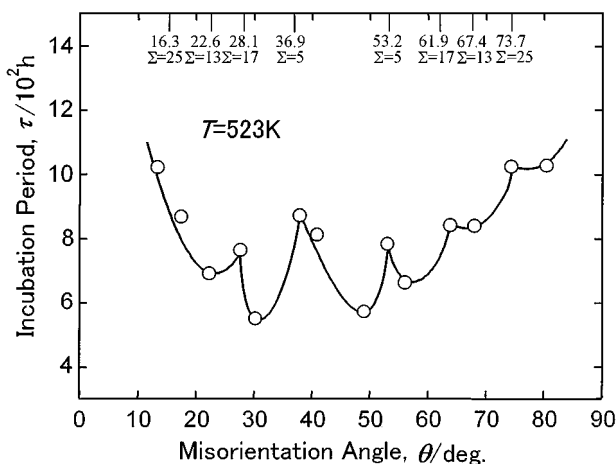


Figure 5 Incubation period  $\tau$  to initiate DP at 523 K, plotted against the misorientation angle  $\theta$ .

$v-\theta$  and  $\tau-\theta$  diagrams agree with those of cusps in the grain-boundary energy  $\gamma-\theta$  curve for Cu reported by Mori *et al.* [9]. Therefore, we conclude that, the higher the boundary energy, the more easily the cell nucleation and growth take place.

In DP processes, generally a grain-boundary cell with a lamellar structure nucleates at a grain boundary and advances into the grain interior. The pucker mechanism proposed by Tu and Turnbull [10] is well known as one of the typical nucleation mechanisms of cells. In this mechanism, a solute-rich phase which has a nearly equilibrium solute concentration first precipitates at a boundary. Since the boundary precipitation of the  $\gamma$  phase is needed for the formation of cell [11], this mechanism is considered applicable to the present alloy. Several investigators [12–15] have reported that such boundary precipitation is easy on random boundaries but difficult on coincidence-site boundaries with low values of  $\Sigma$ , such as 3 and 5. Although the energy of a boundary is not determined only by the  $\Sigma$  values, it is usually assumed that lower- $\Sigma$  boundaries have lower energies. In classical theory, the nucleation rate of precipitates on a boundary is an increasing function of the boundary energy. Also, it appears that an easier migration is achieved on a boundary with a higher energy or a higher- $\Sigma$  value [16, 17]. It may be thus expected that the nucleation and growth of DP occur more easily at a higher-energy boundary. This is actually the case in the present work, as mentioned above.

### 3.3. Cell growth kinetics

In the literature [4, 11], several kinetic methods are available to estimate the grain boundary diffusivity triple product,  $s\delta\tilde{D}_b$  (where  $s$ ,  $\delta$  and  $\tilde{D}_b$  are the segregation factor, boundary thickness and chemical boundary diffusion coefficient, respectively) through the kinetic analysis of DP utilizing the experimentally determined kinetic parameters of  $v$  and  $\lambda$ . The kinetic analysis in the present study to calculate  $s\delta\tilde{D}_b$  has been carried out through the models of Turnbull [18] and Petermann and Hornbogen [19]. According to the Turnbull model

$$s\delta\tilde{D}_b = \frac{x_0}{x_0 - x_e} v\lambda^2 \quad (1)$$

where  $x_0$  is the initial solute content in the alloy and  $x_e$  is the equilibrium solute content in the  $\alpha$  phase. The values of  $x_e$  as a function of  $T$  are reported in the literature [20]. As per the Petermann and Hornbogen model on DP

$$s\delta\tilde{D}_b = \frac{RT}{-8\Delta G} v\lambda^2 \quad (2)$$

where  $\Delta G$  is the driving force for DP in terms of the overall change in the Gibbs energy and  $R$  is the gas constant.  $\Delta G$  consists of the chemical  $\Delta G_c$  and interfacial  $\Delta G_\sigma$  components as follows

$$\Delta G = \Delta G_c + \Delta G_\sigma \quad (3)$$

Assuming ideal solution behaviour,  $\Delta G_c$  for the  $\alpha_0$  to  $\alpha + \gamma$  transformation in DP may be expressed as [4]

$$\Delta G_c = -RT \left[ x_0 \ln \frac{x_0}{x_e} + (1 - x_0) \ln \frac{1 - x_0}{1 - x_e} \right] \quad (4)$$

$\Delta G_\sigma$  for creation of the interlamellar interfaces in DP is given as [4]

$$\Delta G_\sigma = \frac{2\sigma V_m}{\lambda} \quad (5)$$

where  $V_m$  is the molar volume of the  $\alpha_0$  phase and is calculated as  $7.0 \times 10^{-6} \text{ m}^3/\text{mol}$  from the literature [21]. The interfacial energy  $\sigma$  for the  $\alpha$ - $\gamma$  interfaces in the Cu-Be system is not available in the literature. Following Tsubakino *et al.* [7] a value of  $\sigma = 0.4 \text{ J/m}^2$  is used. This value of  $\sigma$  corresponds to the interfacial free energy of a high-angle grain boundary in Cu-base alloys [22].

The temperature dependence of  $s\delta\tilde{D}_b$  is typically expressed in the form of an Arrhenius equation as follows [4]

$$s\delta\tilde{D}_b = (s\delta\tilde{D}_b)_0 \exp\left(-\frac{\tilde{Q}_b}{RT}\right) \quad (6)$$

where  $\tilde{Q}_b$  is the activation energy of chemical grain-boundary diffusion and  $(s\delta\tilde{D}_b)_0$  is the pre-exponential factor. Fig. 6 shows the Arrhenius plots of the respective sets of  $s\delta\tilde{D}_b$  data derived from the models of Turnbull (T) and Petermann and Hornbogen (P-H) for  $\theta = 30^\circ$  boundary, at which the cell growth occurs the most easily in all the boundaries examined in the present study (see Fig. 5). Unfortunately, there are no available data concerning the grain-boundary diffusion process along stationary grain boundaries in this system. For comparison, similar plots for  $s\delta\tilde{D}_b$  data obtained by Tsubakino *et al.* [7] from the T and P-H models for polycrystals of Cu-Be alloys are drawn in Fig. 6. It is seen that both the values of  $s\delta\tilde{D}_b$  for the  $30^\circ$  bicrystals are almost the same as those for the polycrystals. Attempts were made to determine the values of  $s\delta\tilde{D}_b$  derived from the two models for the present Cu-Be alloy polycrys-

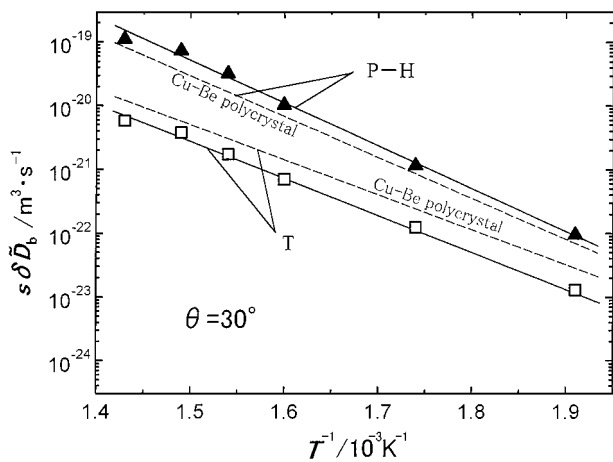


Figure 6 Arrhenius plots of the  $s\delta\tilde{D}_b$  values by using the models of Turnbull (T) [18] and Petermann and Hornbogen (P-H) [19]. The data of Tsubakino *et al.* [7] for Cu-Be polycrystals are given for comparison (dashed lines).

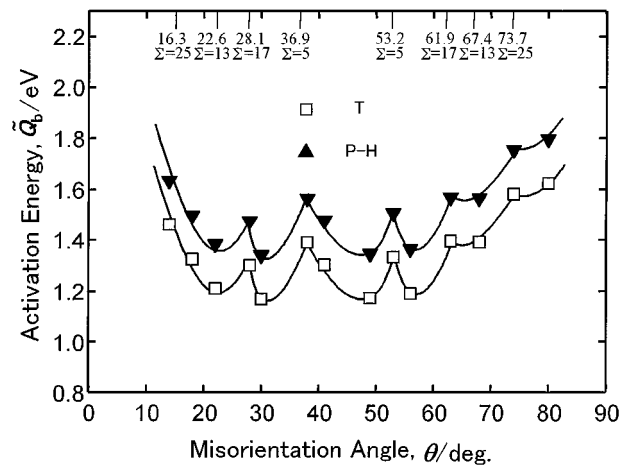


Figure 7 Activation energy  $\tilde{Q}_b$  values for grain-boundary diffusion obtained using the models of T and P-H, plotted against the misorientation angle  $\theta$ .

tals. It was found that for the two models the values were nearly identical to those previously obtained by Tsubakino *et al.* [7]. The values of  $(s\delta\tilde{D}_b)_0$  and  $\tilde{Q}_b$  were determined from the intercept and slope of the straight lines fitted to the  $s\delta\tilde{D}_b$  data, respectively.

Fig. 7 summarizes the values of  $\tilde{Q}_b$  for all the bicrystal specimens examined. For the two models, the  $\tilde{Q}_b$  values show a similar dependence on the misorientation angle; five peaks exist near  $\theta = 28.1^\circ$  ( $\Sigma = 17$ ),  $\theta = 36.9^\circ$  ( $\Sigma = 5$ ),  $\theta = 53.2^\circ$  ( $\Sigma = 5$ ),  $\theta = 61.9^\circ$  ( $\Sigma = 17$ ) and  $\theta = 73.7^\circ$  ( $\Sigma = 25$ ). The  $\tilde{Q}_b$  values determined using the T model [18] lie between 1.2 and 1.6 eV. The values obtained from the P-H model [19] are higher. Since these values of  $\tilde{Q}_b$  are much smaller than that (2.03 eV [23]) of the bulk diffusion of Be in Cu, they can be reasonably identified as the activation energies for boundary diffusion of Be.

The variation of  $\tilde{Q}_b$  with  $\theta$  in Fig. 7 is partly similar to the diffusion of Zn [24] and Bi [25] in [001] symmetric tilt boundaries of Al and Cu, respectively. Aleshin *et al.* [24] measured the diffusivity of Zn in Al boundaries with  $\theta = 10$ - $45^\circ$  and found minima at  $\theta = 23.5^\circ$ ,  $28.5^\circ$  and  $37.0^\circ$ . Yukawa and Sinnott [25] measured the penetration depth of Bi in Cu boundaries parallel to the tilt axis of [001]. The penetration was found to be more difficult for  $22^\circ$ ,  $25^\circ$ ,  $63^\circ$  and  $72^\circ$  boundaries close to  $\theta = 22.6^\circ$  ( $\Sigma = 13$ ),  $\theta = 61.9^\circ$  ( $\Sigma = 17$ ) and  $\theta = 73.7^\circ$  ( $\Sigma = 25$ ) boundaries compared with other high-angle boundaries. The boundary diffusivity- $\theta$  curves reported by Biscondi [26], Uptegrove and Sinnott [27], and Ma and Balluffi [28] were monotonous and showed no clear cusps.

According to the theoretical models of DP, the smaller the activation energy, the larger the cell growth rate becomes. Comparison between Figs 4 and 7 reveals that this is actually the case. Intuitively speaking, it is expected that boundary diffusion in a high-energy boundary is faster than in a low-energy boundary since atoms at the former is considered to be more irregularly arranged. Actually the positions of the cusps and peaks in Figs 4 and 7 are in agreement with those of the energy cusps of the [001] symmetric tilt boundaries in Cu reported by Mori *et al.* [9]. Thus we conclude that a higher-energy boundary has a higher diffusivity.

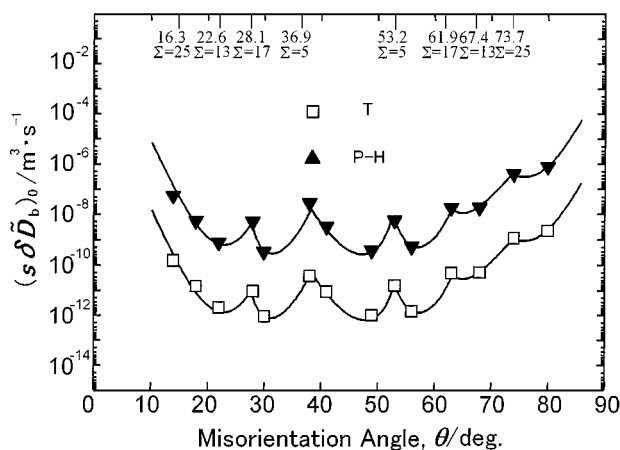


Figure 8  $(s\delta\tilde{D}_b)_0$  values obtained using the T and P-H models, plotted against the misorientation angle  $\theta$ .

The calculated values of  $(s\delta\tilde{D}_b)_0$  are shown against the misorientation angle  $\theta$  in Fig. 8. The  $(s\delta\tilde{D}_b)_0$  values depend strongly on the misorientation. Moreover, it is interesting to note that for the two models, the larger the  $\tilde{Q}_b$  value, the larger is the  $(s\delta\tilde{D}_b)_0$  value.

If grain-boundary diffusion occurs by a vacancy exchange model, the pre-exponential factor is written as  $(s\delta\tilde{D}_b)_0 \propto \exp\{(\Delta S_f + \Delta S_m)/R\}$  from the work by Balluffi [29]. Here  $\Delta S_f$  is the vacancy formation entropy and  $\Delta S_m$  is the vacancy migration entropy. Moreover, according to Shewmon [30], the following empirical relationship often holds;  $\Delta S_f + \Delta S_m \propto \tilde{Q}_b/T_m$  where  $T_m$  is the melting point. From these equations, it can be seen that larger  $\tilde{Q}_b$  results in larger  $(s\delta\tilde{D}_b)_0$ . This relationship is also the case in the present study, as shown in Figs 7 and 8.

#### 4. Conclusions

Studies on the misorientation dependence of DP at [001] symmetric tilt boundaries in Cu-5.2 at% Be alloy bicrystals in the temperature range 523 to 698 K have yielded the following conclusions.

1. A grain boundary migrates at a constant velocity during DP in an isothermal condition, maintaining a constant interlamellar spacing. The interlamellar spacing increases as temperature increases. Both the incubation period for the cell formation and the cell growth rate at a boundary show a good correlation with the energy of the boundary. That is, higher-energy boundaries have a shorter incubation period and a faster growth rate.

2. The grain-boundary diffusion data have been determined through the kinetic analysis of DP using the models of Turnbull [18] and Petermann and Hornbogen [19]. Although the activation energy  $\tilde{Q}_b$  of boundary diffusion varies with the models, the values of  $\tilde{Q}_b$  are smaller than that (2.03 eV) for volume diffusion of Be in Cu. For example, the values estimated by the Turnbull model lie between 1.2 and 1.6 eV, depending on the misorientation. The  $\tilde{Q}_b$  value and pre-exponential factor  $(s\delta\tilde{D}_b)_0$  against misorientation curves display several peaks and the positions of these peaks are in agreement with those of cusps in the boundary energy against mis-

orientation curve. A boundary with a higher energy is described by a smaller value of  $\tilde{Q}_b$  and a smaller value of  $(s\delta\tilde{D}_b)_0$ .

#### Acknowledgements

We would like to thank Professor N. Otsuka, Japan Advanced Institute of Science and Technology, Hokuriku, whose transmission electron microscope was used for the microscopic observation. Mr. H. Okabayashi is also acknowledged for his experimental assistance.

#### References

1. M. FREBEL and J. SCHENK, *Z. Metallk.* **70** (1979) 230.
2. M. MIKI, T. YAMASAKI, N. UYAMA and Y. OGINO, *J. Japan Inst. Metals* **53** (1989) 388.
3. T. SHIBAYANAGI, Y. KITAZUME and S. HORI, *ibid.* **54** (1990) 131.
4. I. KAUR, Y. MISHIN and W. GUST, "Fundamentals of grain and interphase boundary diffusion," 3rd ed. (John Wiley & Sons, Chichester, 1995) p. 303.
5. I. MANNA, W. GUST and B. PREDEL, *Scripta Metall. Mater.* **24** (1990) 1635.
6. I. MANNA, J. N. JHA and S. K. PABI, *J. Mater. Sci.* **30** (1995) 1449.
7. H. TSUBAKINO and R. NOZATO, *J. Japan Inst. Metals* **43** (1979) 42.
8. H. TSUBAKINO, R. NOZATO and A. YAMAMOTO, *Mater. Sci. Tech.* **9** (1993) 288.
9. T. MORI, T. ISHII, M. KAJIHARA and M. KATO, *Phil. Mag. Lett.* **75** (1997) 367.
10. K. N. TU and D. TURNBULL, *Acta Metall.* **15** (1967) 369.
11. D. B. WILLIAMS and E. P. BUTLER, *Inter. Metals Rev.* **26** (1981) 153.
12. P. N. T. UNWIN and R. B. NICHOLSON, *Acta Metall.* **17** (1969) 1379.
13. E. P. BUTLER and P. R. SWANN, *ibid.* **24** (1976) 343.
14. P. CZURRATIS, R. KROGGEL and H. LÖFFER, *Z. Metallk.* **79** (1988) 307.
15. R. MONZEN, K. KITAGAWA, M. KATO and T. MORI, *J. Japan Inst. Metals* **54** (1990) 1308.
16. J. W. RUTTER and K. T. AUST, *Acta Metall.* **13** (1965) 181.
17. E. M. FRIDMAN, C. V. KOPEZKY and L. S. SHVINDLERMAN, *Z. Metallk.* **66** (1975) 533.
18. D. TURNBULL, *Acta Metall.* **3** (1955) 55.
19. J. PETERMANN and E. HORNBOGEN, *Z. Metallk.* **59** (1968) 814.
20. T. B. MASSALSKI (Editor-in chief), "Binary Alloy Phase Diagrams" (ASM International, Materials Park, Ohio, 1992) p. 645.
21. H. TANIMURA and G. WASSERMANN, *Z. Metallk.* **25** (1933) 179.
22. M. C. INMAN and H. R. TIPLER, *Met. Rev.* **8** (1963) 105.
23. R. L. FOGEL'SON, YA. A. UGAY, A. V. POKOYEV, I. A. AKIMOVA and V. D. KRETININ, *Phys. Metall. Metallogr.* **35** (1973) 176.
24. A. N. ALESHIN, B. S. BOKSHEIN and L. S. SHVINDLERMAN, *Sov. Phys. Sol. State* **19** (1977) 2051.
25. S. YUKAWA and M. J. SINNOTT, *Trans. Amer. Inst. Mining Eng.* **215** (1959) 338.
26. M. BISCONDI, in "Physical Chemistry of the Solid States: Applications to Metals and their Compounds," edited by P. Lacombe (Elsevier, Amsterdam, 1984) p. 225.
27. W. R. UPTHEGROVE and M. J. SINNOTT, *Trans. Amer. Soc. Metals* **50** (1958) 1031.
28. Q. MA and R. W. BALLUFFI, *Acta Metall. Mater.* **41** (1993) 133.
29. R. W. BALLUFFI, *Metall. Trans. A* **13** (1982) 2069.
30. P. G. SHEWMON, "Diffusion in Solids" (McGraw-Hill, New York, 1963) p. 44.

Received 1 December 1999  
and accepted 8 May 2000